ORIGINAL ARTICLE

Ultrastructure and Molecular Phylogenetic Position of *Heteronema scaphurum*: A Eukaryovorous Euglenid with a Cytoproct

Susana A. Breglia[1], Naoji Yubuki & Brian S. Leander

Canadian Institute for Advanced Research, Program in Integrated Microbial Biodiversity, Departments of Zoology and Botany, University of British Columbia, 6270 University Boulevard, Vancouver, BC, V6T 1Z4, Canada

ABSTRACT

Euglenids comprise a distinct clade of flagellates with diverse modes of nutrition, including phagotrophy, osmotrophy and phototrophy. Much of the previous research on euglenids has focused on phototrophic species because of their ecological abundance and significance as indicators for the health of aquatic ecosystems. Although largely understudied, phagotrophic species probably represent the majority of euglenid diversity. Phagotrophic euglenids tend to be either bacterivorous or eukaryovorous and use an elaborate feeding apparatus for capturing prey cells. We characterized the ultrastructure and molecular phylogenetic position of *Heteronema scaphurum*, a eukaryovorous euglenid collected in freshwater. This species was equipped with a distinct cytoproct through which waste products were eliminated in the form of faecal pellets; a cytoproct has not been reported in any other member of the Euglenida. *Heteronema scaphurum* also had a novel predatory mode of feeding. The euglenid ensnared and corralled several green algal prey cells (i.e. *Chlamydomonas*) with hook-like flagella covered in mucous before engulfing the bundle of prey cells whole. Molecular phylogenetic analyses inferred from small subunit rDNA sequences placed this species with other eukaryovorous euglenids, which was consistent with ultrastructural features associated with the feeding apparatus, flagellar apparatus, extrusomes, and pellicle.

THE Euglenida is a diverse group of flagellates unified by both ultrastructural and molecular features. Euglenids share a distinctive pellicle that is formed by the plasma membrane, interlocking proteinaceous strips, subtending microtubules, and cisternae of endoplasmic reticulum (Esson and Leander 2006; Leander and Farmer 2000; Leander et al. 2007). Different modes of nutrition in the group (phagotrophy, osmotrophy and phototrophy) correlate with the number of strips and the degree of plasticity in the pellicle (Leander and Farmer 2000, 2001a; Leander et al. 2001a). Bacterivorous species tend to have rigid cells with few (less than 16) longitudinally arranged strips, whereas eukaryovorous species tend to have a larger number (16 or more) of helically arranged strips on the cell surface; eukaryovorous species also tend to distort their cell shape in a manner that is characteristic of euglenids called "euglenoid movement" or "metaboly" (Leander et al. 2001b; Triemer and Farmer 1991; Triemer et al. 2006). This ability, coupled with the presence of a well-developed feeding apparatus consisting of microtubule-based rods and vanes, allows eukaryovorous species (e.g. *Peranema*,

Dinema, and *Urceolus*) to capture and engulf large prey cells, such as microalgae. The engulfment of a green algal prey cell led to a secondary endosymbiotic event, which gave rise to a distinct clade of phototrophic euglenids (Gibbs 1978, 1981; Leander 2004; Leander et al. 2007; Rogers et al. 2007; Yamaguchi et al. 2012).

Phagotrophic euglenids typically have two emergent flagella that are used to glide along substrates: one oriented straight in front of the cell (the anterior or dorsal flagellum) and the other that curves backwards and trails behind the cell (the posterior or ventral flagellum). One of the more common phagotrophic genera is *Heteronema*, which is found in both freshwater and marine environments; about 43 species have been described so far (Schroeckh et al. 2003). *Heteronema* is morphologically very similar to *Peranema* under the light microscope; both lineages are metabolic, capable of gliding, possess conspicuous feeding rods within the anterior end of the cell, and have an anterior flagellum that is longer and thicker than the posterior flagellum (Lee et al. 2005). However, unlike *Peranema*, the posterior flagellum of

Heteronema does not stick closely to the ventral side of the cell. To date, members of this genus have only been studied with light microscopy. Here, we characterize the eukaryovorous euglenid *Heteronema scaphurum* using not only light microscopy and video analysis, but also scanning electron microscopy, transmission electron microscopy, and molecular phylogenetic analysis of SSU rDNA sequences. Our study demonstrated that this species has a distinct and novel feeding behaviour involving hook-like flagella and a mucilaginous web that captures (green algal) prey before engulfing the cells whole. *Heteronema scaphurum* also eliminates remnant prey material as faecal pellets through a novel cytoproct. The discovery of these novel features in this species expands our knowledge of euglenid diversity, especially with regard to phagotrophic species, and provides improved context for understanding the eukaryovorous origins of phototrophic euglenids.

MATERIALS AND METHODS

Cell isolation and cultivation

A sample of freshwater sediments from a pond in Illinois, USA, was collected during the Spring of 2007, and a culture was established at room temperature in a 0.01% Knop medium (Saito et al. 2003) using *Chlamydomonas* as prey cells.

Light microscopy and video analysis

Differential interference contrast (DIC) light micrographs (LMs) were taken using a Zeiss Axioplan 2 imaging microscope (Carl Zeiss Microscopy GmbH, Jena, Germany) and a Leica DC500 digital chilled CCD camera (Leica Microsystems Digital Imaging, Cambridge, U.K.). Cells were fixed with 1% (v/v) glutaraldehyde for high magnification observations. Digital videos were taken with a PixeLink Megapixel colour digital camera (LixeLink, Ottawa, ON, Canada) connected to a Zeiss Axiovert 200 inverted microscope (Carl Zeiss Microscopy GmbH).

Electron microscopy

Cells were fixed for SEM using a 4% osmium tetroxide vapour protocol described previously (Leander and Farmer 2000). The cells were then transferred onto a 10 μm polycarbonate membrane filter, dehydrated with a graded ethanol series, and critical point dried with CO_2 using a Tousimis Critical Point Dryer. The filter was then mounted on an aluminium stub, sputter coated with gold/palladium using a Cressington 208HR High Resolution Sputter Coater (Cressington Scientific Instruments Ltd., Watford, England), and observed with a Hitachi S-4700 field emission scanning electron microscope (Hitachi High Technologies Corp., Tokyo, Japan).

Cells were fixed for transmission electron microscopy (TEM) using 2% glutaraldehyde in 0.1 M sodium cacodylate buffer (SCB). The fixed cells were washed in 0.1 M SCB three times, and postfixed in 1% (w/v) osmium tetroxide in 0.2 M SCB, in ice, for 1 h. The cells were then dehydrated through a graded series of ethanol and 100% acetone, and infiltrated with a graded series of acetone-Epon 812 resin mixtures and 100% Epon 812 resin. Ultra-thin sections were collected on copper Formvar-coated slot grids, stained with 2% (w/v) uranyl acetate and lead citrate (Reynolds 1963), and observed using a Hitachi H7600 electron microscope.

Brightness and contrast of all micrographs were adjusted, as well as labelled and assembled into plates, using Photoshop CS4.

DNA extraction and PCR amplification

Total genomic DNA was extracted using the MasterPure Complete DNA and RNA purification Kit (Epicentre, Maddison, WI; Catalogue number MC85200) from ~ 30 cells, following the procedures provided by the manufacturer. Polymerase chain reactions (PCR) of 18S rDNA were performed using PuRe Taq Ready-To-Go PCR beads kit (GE Healthcare, Buckinghamshire, U.K.), and the following primers: 5′-TGCGCTACCTGGTTGATCC-3′ and 5′-AACGGAATYAACCA GACARAT-3′. Amplified DNA fragments were purified from agarose gels using UltraClean 15 DNA Purification Kit (MO Bio, Carlsbad, CA), and subsequently cloned into the TOPO TA Cloning Kit (Invitrogen, Carlsbad, CA). Three clones were sequenced with the ABI Big-Dye reaction mix using the vector primers and three internal primers: Dinema18s1R (5′-GGACTACGACGGTATCTGATCAT-3′), 475EugF (5′- AAGTCT GGTGCCAGCAGCYGC-3′) and DinemaSSU620F (5′- GCAA GACAGCTGTGCGATAGCAA-3′). The new sequence was screened with BLAST, identified by molecular phylogenetic analyses, and submitted to the GenBank database (JN566139).

Multiple sequence alignment and molecular phylogenetic analyses

We obtained a 2,860 bp sequence that corresponded to positions 380–1687 of *Euglena gracilis*. The new 18S rDNA sequence was analysed within the context of a 39-taxon alignment consisting of taxa representing the Euglenozoa (636 unambiguously aligned sites). Ambiguously aligned positions and gaps were excluded.

Molecular phylogenetic relationships were inferred using maximum likelihood (ML) and Bayesian inference (BI) methods with PhyML v2.4.5 (Guindon and Gascuel 2003) and MrBayes v3.1.1 (Ronquist and Huelsenbeck 2003), respectively, with the graphical interface TOPALi v2.5 (Milne et al. 2009). The models used for ML and BI to generate phylogenetic trees were chosen using Model selection in TOPALi v2.5 (Milne et al. 2009). In both cases, the nucleotide dataset was analysed using a general-time-reversible (GTR) model of base substitutions, plus a gamma correction (gamma value = 0.663) with eight substitution rate categories and a proportion of invariable sites = 0.165 (GTR + I + G). ML bootstrap analysis of 100 replicates was performed with the same param-

eters described above. For the BI, the program MrBayes was set to operate with four Monte-Carlo-Markov chains (MCMC) (default temperature = 0.2). A total of 1,000,000 generations was calculated with trees sampled every 50 generations, resulting in 20,000 trees saved. A 10% burn-in was applied, resulting in 18,000 trees used (i.e. 2,000 sampled trees were discarded).

RESULTS

General morphology

The cells were spindle-shaped with a tapering posterior end, 45–70 μm long and approximately 30 μm wide (*n* = 250). A vestibular opening was located at the ante-

rior end of the cell, which led to a flagellar pocket (FP) and to a feeding pocket (Fe) (Fig. 1, 2). The posterior end of the cell contained a distinct concavity, or "cytoproct", through which material was periodically released (Fig. 3–7, 11–13). Two heterodynamic flagella emerged from the vestibular opening (Fig. 1–5, 8). The dorsal (anterior) flagellum (DF) was approximately the same length as the cell body (~ 60 μm long) and extended straight forward while gliding; the ventral (posterior) flagellum (VF) was slightly shorter, about 0.7 times the cell length, and trailed freely beneath the cell. Both flagella were adorned with hairs (Fig. 8–10). The cells were capable of euglenoid movement and glided smoothly, with the anterior flagellum extended in front of the cell and probing the substrate, and with the ven-
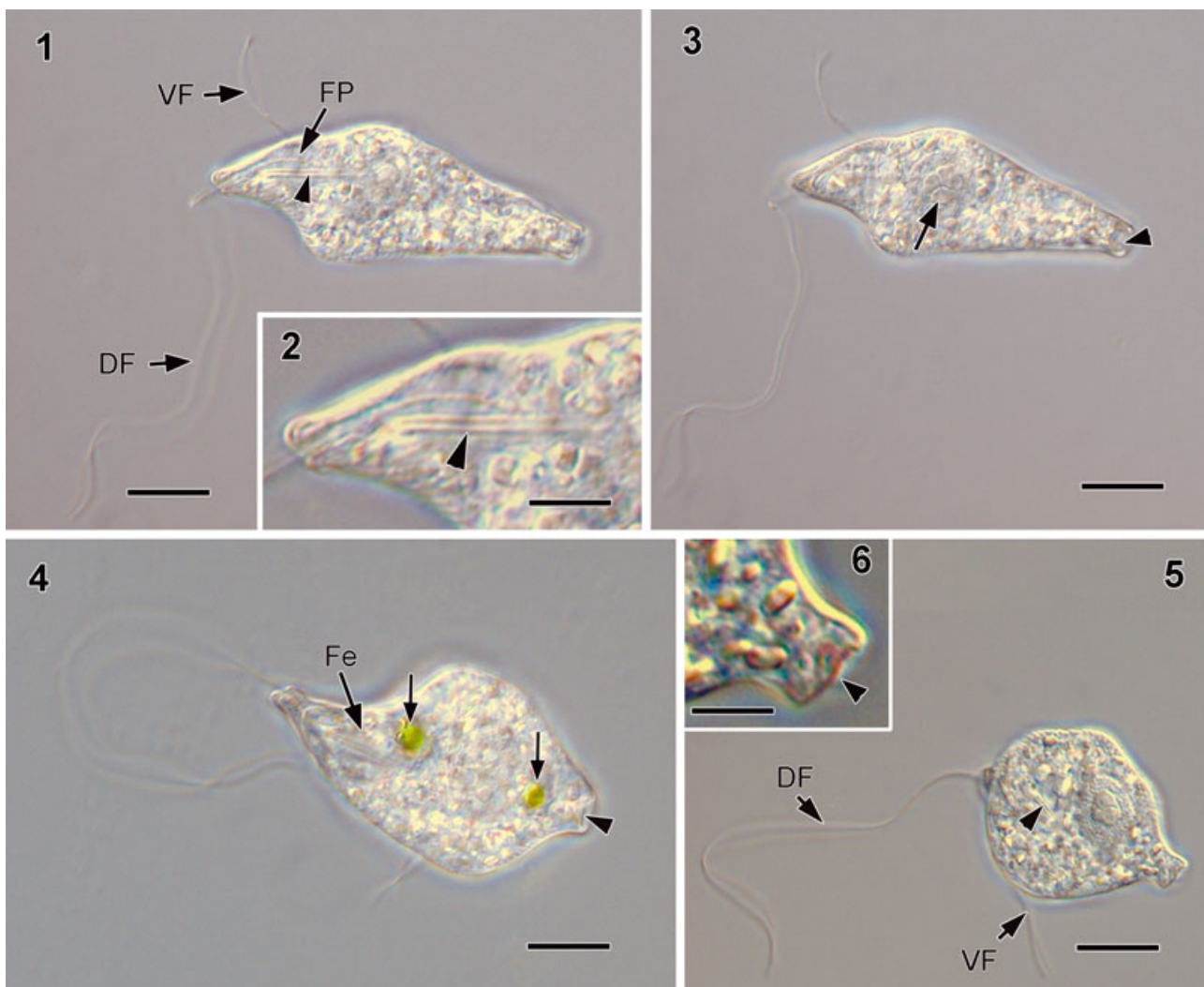
Fig. 1–6. Light micrographs showing fixed cells of *Heteronema scaphurum*. **1.** Side view showing dorsal and ventral flagella (DF and VF respectively), flagellar pocket (FP) and feeding apparatus (arrowhead). Scale bar = 10 μm. **2.** High magnification view showing feeding apparatus (arrowhead). Scale bar = 5 μm. **3.** Side view showing the nucleus with endosomes (arrow) and cytoproct (arrowhead). **4.** Cell in dorsal view showing the feeding pocket (Fe), engulfed prey *Chlamydomonas* (arrows), and cytoproct (arrowhead). **5.** Dorsal-posterior view showing the dorsal flagellum (DF) and the ventral flagellum (VF), and the feeding apparatus (arrowhead). Scale bars 3–5 = 10 μm. **6.** Detail of Fig. 5 showing the cytoproct, and material being excreted (arrowhead). Scale bar = 5 μm.
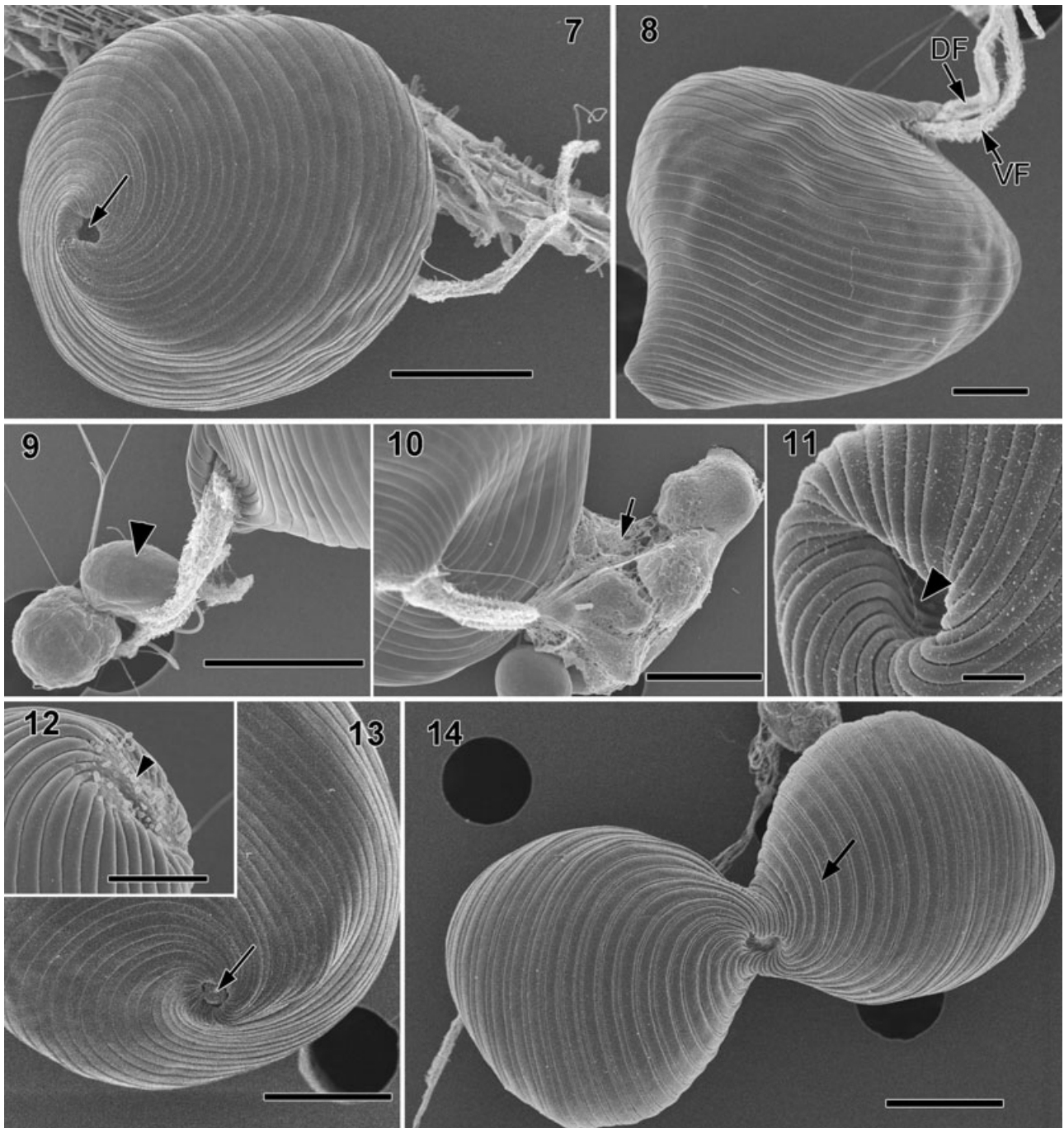
Fig. 7–14. Scanning electron micrographs of *Heteronema scaphurum*. **7.** Posterior view of a cell showing the cytoproct (arrow). Scale bar = 10 μm. **8.** Lateral view of the cell showing the dorsal and ventral flagella with mastigonemes (DF and VF respectively). Scale bar = 5 μm. **9.** Ventral view of the anterior tip of a cell showing two prey cells (*Chlamydomonas*, arrowhead) that have been captured by both flagella of the euglenid. Scale bar = 10 μm. **10.** Anterior view of a cell showing a mucus web (arrow) surrounding the prey cells. Scale bar = 10 μm. **11.** Posterior tip of a cell showing pellicle strips extending into the cytoproct (arrowhead). Scale bar = 1 μm. **12.** Posterior tip of a cell showing material being secreted from the cytoproct. Scale bar = 5 μm. **13.** Posterior view of a cell showing a faecal pellet (arrow) being secreted through the cytoproct. Scale bar = 10 μm. **14.** Posterior view of a cell dividing along its antero-posterior axis. The arrow shows the thinner nascent pellicle strips. Scale bar = 10 μm.

tral flagellum bent backwards beneath the cell. The cell divided from anterior to posterior along the longitudinal axis (Fig. 14).

Feeding behaviour

Heteronema scaphurum devoured *Chlamydomonas*. During this process, both flagella participated in the capture of prey cells; the dorsal flagellum formed an arc, hooked several prey cells, and pushed them towards the vestibular opening (Fig. 15–20). The ventral flagellum participated in the capture and manipulation of the prey cells by trapping the cells within the arc formed by the dorsal flagellum. The cell also secreted a sticky substance that functioned to envelope the prey within a web of mucus (Fig. 9, 10). Once the prey cells were moved against the vestibular opening, the anterior end of the cell expanded as the flagella continued to push the prey inwards (Fig. 16–20). Then the microtubular rods that separate the flagellar and the feeding pockets pushed the flagella to one side, preventing the passage of food into the flagellar pocket and, at the same time, enlarging the feeding cavity, as the prey cells were ingested whole. During this process, *H. scaphurum* also distorted its shape, presumably to generate forces required to facilitate the engulfment of the prey

(Fig. 19, 20). The entire process of feeding, from prey capture to engulfment, took approximately one minute to complete.

We also observed material that was released through the posterior cytoproct during the feeding process (Fig. 6, 12, 13). The cells were able to discharge either mucilaginous material (Fig. 12) or solid faecal pellets around 3 μm in diameter (Fig. 13). The faecal pellets accumulated and were easily observed in the culture dishes.

Cell surface

Heteronema scaphurum had 28 pellicle strips ($n = 100$) that ran along the antero-posterior axis of the cell and formed a helically arranged pattern on the cell surface (Fig. 7–14). All of the strips were approximately the same width; there was no ventral groove or "flagellar strip" containing the ventral flagellum. All of the strips extended into the anterior vestibulum and the posterior cytoproct; there were no indications of strip reduction on either end of the cell (Fig. 7, 9–14). The number of strips doubled prior to cytokinesis, whereby new thinner strips emerged between the parental thicker strips (Fig. 14). The transverse ultrastructure of the pellicle consisted of the plasma membrane, relatively thick (100 nm wide)
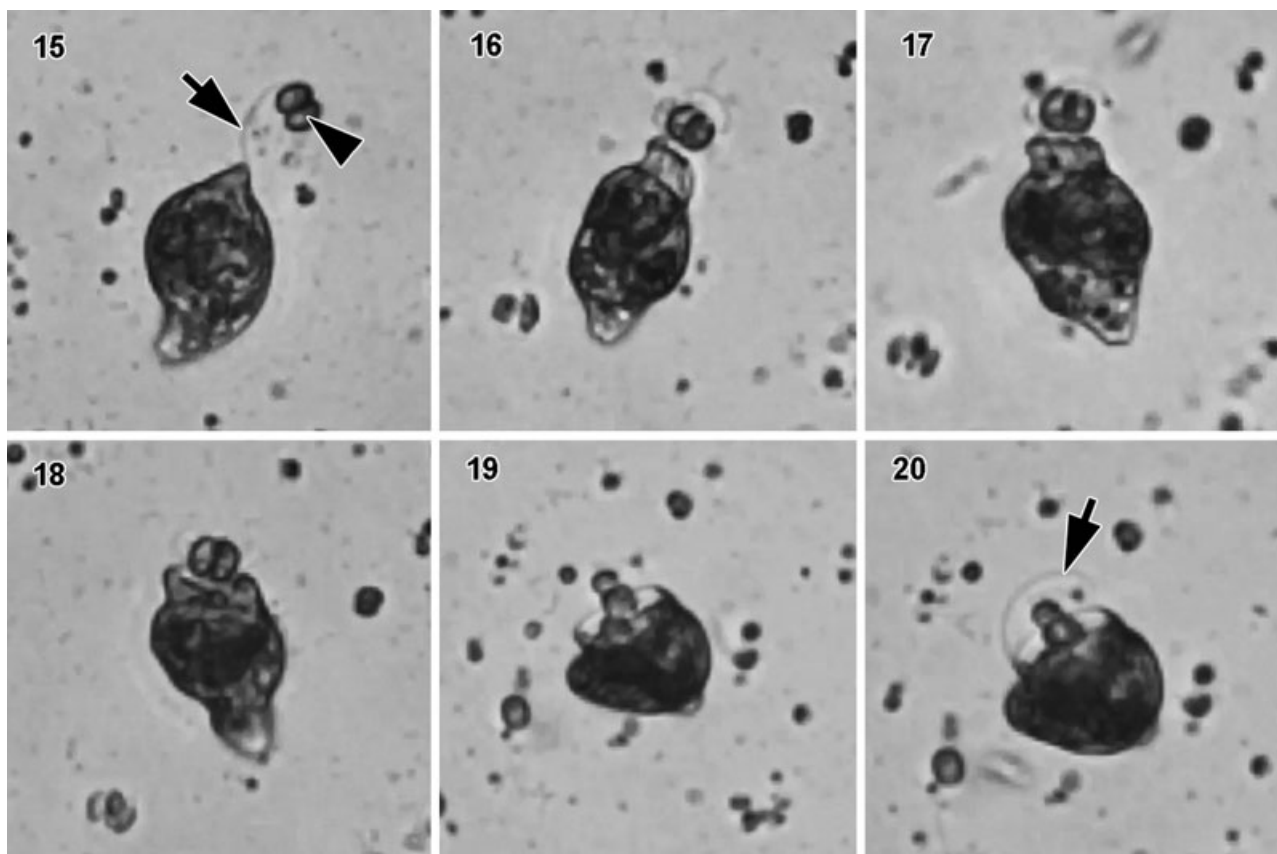
Fig. 15–20. Time series of video microscope images of *Heteronema scaphurum* feeding on the green alga *Chlamydomonas*. The dorsal flagellum (arrow) captures and guides the prey (arrowhead) towards the vestibular opening. Once in contact with the prey, the vestibular opening of the cell expands, the flagella thrust the prey cells inwards, and the whole prey cells are engulfed.
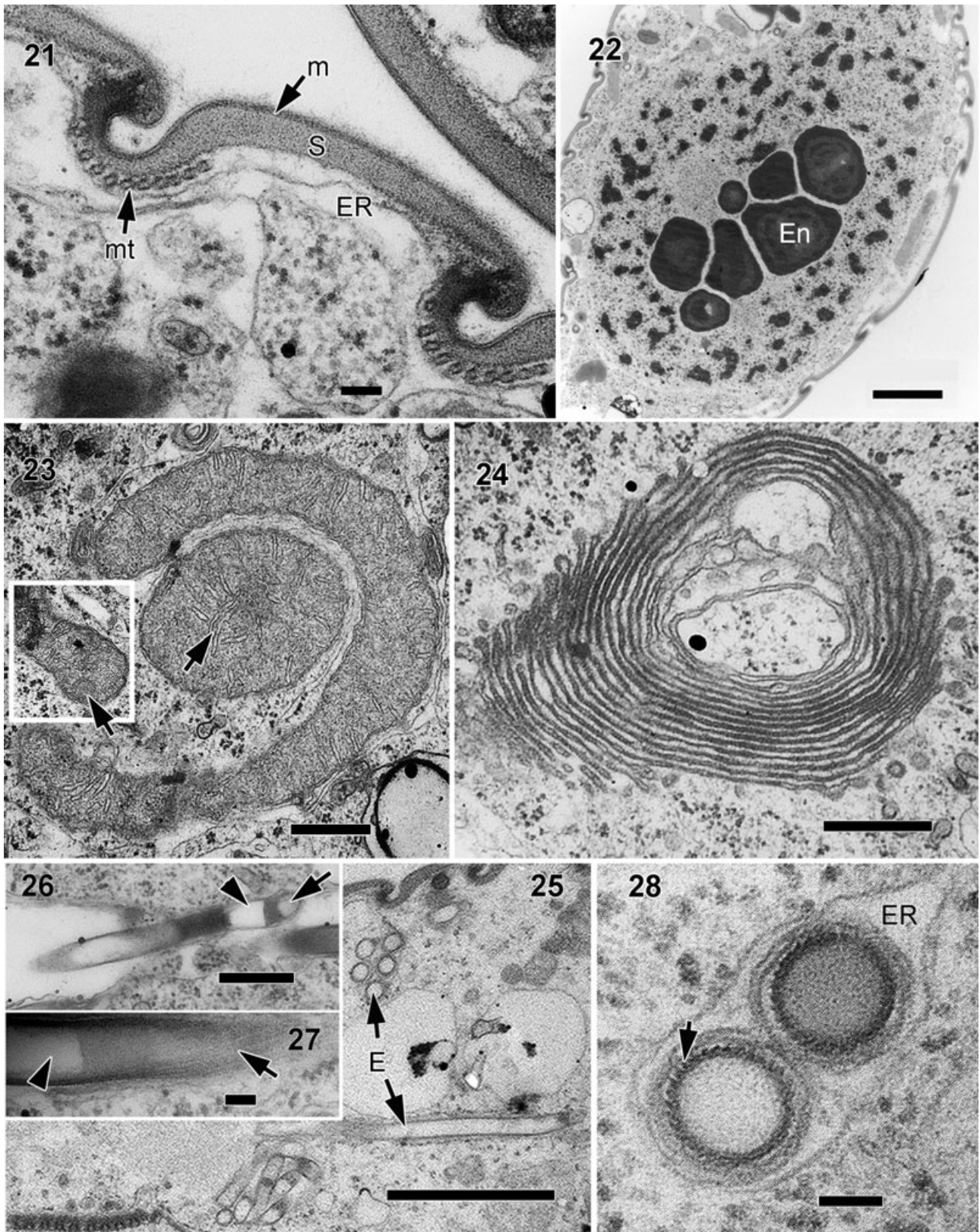
Fig. 21–28. Transmission electron micrographs of *Heteronema scaphurum*. **21.** Cross-section through the pellicle showing the plasma membrane (m), thick proteinaceous strips (S), microtubules (mt), and cisternae of endoplasmic reticulum (ER). Scale bar = 100 nm. **22.** Micrograph showing the nucleus containing profiles of several conspicuous endosomes (En) and permanently condensed chromosomes. Scale bar = 2 μm. **23.** Mitochondria with discoidal cristae (arrows). Scale bar = 500 nm. **24.** Golgi bodies. Scale bar = 500 nm. **25.** Longitudinal and cross-section views of tubular extrusomes (E). Scale bar = 2 μm. **26.** Longitudinal section of an extrusome showing an anterior clear "cup" (arrowhead) with operculum (arrow). The region next to the cup, of approximately 200 nm in length, appears granular and darker than the rest of the tube. Scale bar = 500 nm. **27.** Detail of extrusome in longitudinal view, showing a striated outer region (arrow) and a clear, hollow core (arrowhead). Scale bar = 100 nm. **28.** Cross-section of extrusomes at different levels showing a dark and helically striated outer region (arrow), and a granular core. Scale bar = 100 nm.

S-shaped proteinaceous strips, a discontinuous row of microtubules beneath the heel of each strip, and cisternae of endoplasmic reticulum (ER) (Fig. 21). The number of microtubules underlining the strips was typically 10, but varied from three to more than 18. The strips had an uneven thickness, becoming thinner towards the zone of articulation with the next strip. The arch terminated with a conspicuous overhang that connected to the hook of the adjacent strip by three bridges in the articulation zone (see Leander and Farmer 2001b for definitions of terminology).

Cytoplasmic organelles

Light and transmission electron micrographs showed a single nucleus with permanently condensed chromosomes and several conspicuous, centrally located, endosomes (Fig. 3, 22). The mitochondria had discoidal cristae (Fig. 23), and robust Golgi bodies were formed of many concentric cisternae (Fig. 24). Tubular extrusomes were positioned immediately beneath the articulation zones between S-shaped pellicle strips and throughout the cytoplasm, sometimes forming batteries of parallel units (Fig. 25). The resting tubular extrusomes were approximately 2.7 μm long and 0.2 μm wide (Fig. 25–27). The extrusomes were circular in cross-section, with a darkly stained outer region surrounding a granular core (Fig. 26–28) and had helically arranged surface striations. The core contained an anterior (clear) "cup" followed by a granular dark band about 200 nm long and a lighter (apparently hollow) core (Fig. 26–28).

Feeding apparatus

The vestibular opening (V) at the anterior end of the cell led to the flagellar pocket (Fe), as well as to the feeding pocket (FP). The dorsal wall of the vestibulum was reinforced by dense fibrous material (Fig. 29). The feeding apparatus itself consisted of four structures: a dorsal rod (DR), a ventral rod (VR), an accessory rod (AR), and four "vanes" (i.e. a single row of microtubules affixed to a membrane). It was positioned between the feeding pocket and the anterior region of the flagellar pocket, separating them (Fig. 33, 34), and extended beyond the flagellar pocket for approximately one-third of the cell length (Fig. 31–33). The accessory rod interacted with the ventral rod and the wall of the feeding pocket. A group of microtubules lined the dorsal side of the feeding pocket and supported a cluster of hairs ("tomentum") that extended into it (Fig. 29, 30, 33). The rods were formed of interlinked microtubules embedded

in an amorphous matrix (Fig. 35–37). At the posterior end, these were entirely formed of microtubules embedded in a thin homogeneous matrix (Fig. 35); at the anterior end, the rods contained microtubules within a heterogeneous matrix that formed a conspicuous peripheral ring in transverse sections (Fig. 29–31, 37).

The accessory rod was composed of only a few microtubules embedded in a dense amorphous matrix (Fig. 38, 39). It also had a lamellar projection that extended towards the anterior end of the cell (Fig. 39). At the most anterior level of the feeding apparatus, the lamellar projection of the accessory rod connected to a microtubule-lined ventral lamella (VL) that extended inwards from the wall of the vestibulum (Fig. 29, 30, 33). The ventral lamella arched over the feeding pocket and joined the dorsal lamella (DL) (Fig. 33). Near the anterior end of the cell, both the dorsal and ventral rods were connected to one another. Near the posterior end of the cell, the rods were also connected, forming one microtubular bundle that was compartmentalized by the four vanes (Fig. 35). A series of more anterior sections through the rods demonstrate the detachment of the vanes from the rods (Fig. 36, 37). A striated fibre (SF) lined the dorsal-right side of the feeding pocket (Fig. 33, 34, 45). A row of microtubules was positioned on both sides of this fibre: four microtubules to the right, and eight to more than eighteen microtubules on the left.

Flagellar apparatus

Details of the flagellar apparatus structures are shown in Fig. 40–46. The flagellar pocket merged with the feeding pocket near the anterior end of the cell, forming the vestibulum. Two heterodynamic flagella emerged from the base of the flagellar pocket, which was reinforced by electron-dense material near the vestibular opening (Fig. 43). Each flagellum had axonemes with the typical 9 + 2 arrangement of microtubules (Fig. 42). Near the transition zone, which appeared swollen, the two central microtubules were absent, showing a 9 + 0 arrangement (Fig. 40). Both flagella also contained paraxonemal rods (PR) (Fig. 40–42) and conspicuous flagellar hairs (mastigonemes) (Fig. 42). The paraxonemal rods in the dorsal flagellum had a whorled disposition in transverse section; the paraxonemal rods in the ventral flagellum had a lattice of parallel fibres in transverse section (Fig. 41, 42). A striated system of hairs connected the two flagella near the vestibular opening (Fig. 42).

Like in other euglenids, the flagellar apparatus consisted of two basal bodies and three microtubular roots. The fla-
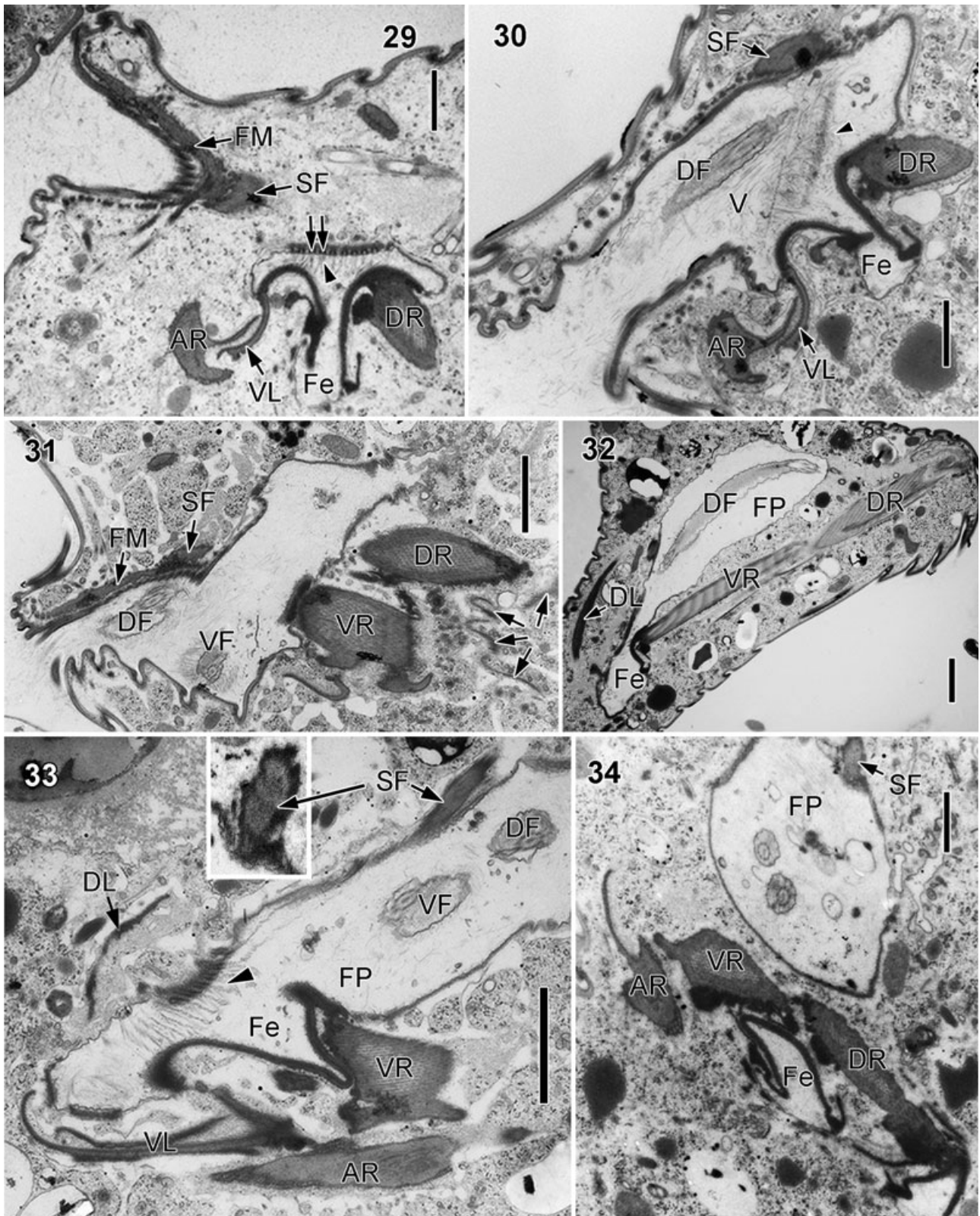
Fig. 29–34. Transmission electron micrographs showing the feeding apparatus in *Heteronema scaphurum* at different levels along the longitudinal axis of the cell. **29.** Cross-section through the anterior end of the cell showing part of the feeding pocket (Fe), the dorsal rod (DR) and the accessory rod (AR). The accessory rod has a lamellar expansion that connects with a microtubule-lined ventral lamella (VL) extending from the wall of the feeding pocket. Microtubules line the dorsal side of the feeding pocket (arrows). A cluster of hairs or "tomentum" (arrowhead) extends from the dorsal microtubules and into the feeding pocket. FM = fibrous material lining the anterior pocket of the cell; SF = striated fibre. Scale bar = 1 μm. **30.** Transversal section showing the enlarged vestibulum (V) formed by the merging of the flagellar pocket and the feeding pocket. A cluster of hairs (arrowhead) still demarcates the deeper separation of the flagellar region and the feeding pocket (Fe). DF = dorsal flagellum. Scale bar = 1 μm. **31.** Cross-section at the anterior end of the cell. The region of the vestibulum that is continuous with the flagellar pocket is reinforced by fibrous material (FM) and a striated fibre (SF). Both dorsal and ventral rods (DR and VR respectively) are visible, as well as the vanes of the feeding apparatus (arrows). VF = ventral flagellum. Scale bar = 1 μm. **32.** Oblique section showing the position of the dorsal and ventral rods (DR and VR respectively) relative to the feeding pocket (Fe) and the flagellar pocket (FP). DF = dorsal flagellum; DL = dorsal lamella. Scale bar = 2 μm. **33.** Semi-longitudinal section of the flagellar pocket (FP) and the feeding pocket (Fe). The ventral lamella (VL) arches over the feeding pocket and connects to the dorsal lamella (DL). The arrowhead shows the cluster of hairs lining the feeding pocket. AR = accessory rod; DF = dorsal flagellum; SF = striated fibre; VF = ventral flagellum; VR = ventral rod. Scale bar = 2 μm. **34.** Separation of the feeding pocket (Fe) from the flagellar pocket (FP). AR = accessory rod; DR = dorsal rod; SR = striated fibre; VR = ventral rod. Scale bars = 1 μm.
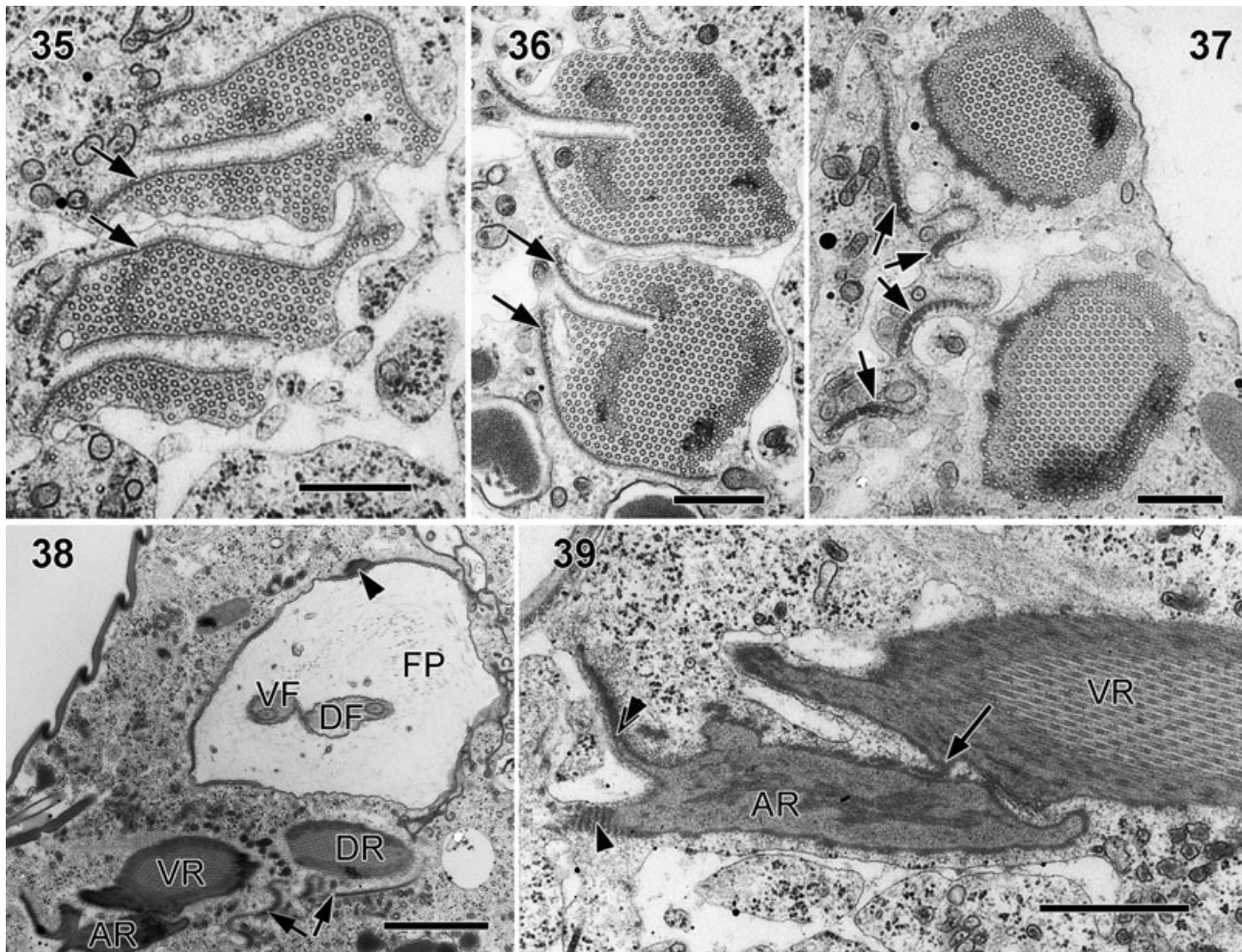
Fig. 35–39. Transmission electron micrographs showing the feeding apparatus in *Heteronema scaphurum*. **35–37.** Non-consecutive serial cross-sections through the rods. Scale bars = 500 nm. **35.** A posterior section through the rods showing that they are connected, forming a single structure entirely formed by microtubules embedded in a homogeneous matrix. Deep grooves in the microtubular bundle are lined by four vanes (arrows). **36.** A more anterior section through the rods showing separate bundles of microtubules embedded in a more heterogeneous matrix. There are still grooves in the microtubular bundles associated with the four vanes. **37.** An anterior section through the rods showing the detachment of the vanes (arrows) from the rods. **38.** Cross-section showing the relationship of the flagellar pocket (FP) and the feeding apparatus. The rods are separated from the flagellar pocket and the vanes. Arrowhead: striated fibre; AR = accessory rod; DF = dorsal flagellum; DR = dorsal rod; VF = ventral flagellum; VR = ventral rod. **39.** Detail of the connection (arrow) between the ventral rod (VR) and the accessory rod (AR). The arrowhead shows a striated fibre extending towards the pellicle. The double arrowhead shows the ventral lamella. Scale bars in 38–39 = 1 μm.

Fig. 40–46. Transmission electron micrographs of the flagellar apparatus of *Heteronema scaphurum*. **40.** Cross-section through the swollen flagellar transition zone, showing a 9 + 0 arrangement of microtubules (arrow). PR = paraxial rod. Scale bar = 100 nm. **41.** Oblique section through the dorsal and ventral flagella (DF and VF respectively) showing the paraxial rods (arrows) and mastigonemes (arrowheads). Scale bar = 500 nm. **42.** Cross-section of the flagella (DF = dorsal flagellum; VF = ventral flagellum) showing the 9 + 2 arrangement of axonemal microtubules and the paraxial rods (arrows). The paraxial rod in the DF has a whorled disposition, and the paraxial rod in the VF is composed of a lattice-like pattern of fibres. A striated fibril (arrowhead) connects both flagella near the posterior end of the flagellar pocket. Scale bar = 100 nm. **43.** Cross-section through the flagellar pocket at the anterior level showing the dorsal flagellum (DF), the ventral flagellum (VF), and pellicle strips (arrows) extending into the flagellar pocket, which is lined by fibrous material (FM). Scale bar = 500 nm. **44.** Cross-section through the flagellar pocket at the level of the flagellar transition zones showing the three microtubular roots: the dorsal flagellar root (dr) is associated with the dorsal basal body; the ventral and intermediate roots (vr and ir respectively) are associated with the ventral basal body. DR = dorsal rod; VR = ventral rod. Scale bar = 500 nm. **45.** Cross-section through the middle part of the flagellar pocket. The dorsal flagellar root (dr) is formed by microtubules that extend along the dorsal side of the flagellar pocket. The intermediate flagellar root (ir) is positioned between the dorsal and the ventral roots, supporting the left side of the flagellar pocket. The ventral root (vr) initially consists of four microtubules, supporting the ventral side of the pocket. A striated fibre (SF) reinforces the dorsal side of the pocket. Rows of microtubules lie on both sides of SF: four microtubules on the left (arrowhead) and sixteen linked microtubules (LMt) on the right side of striated fibre. DR = dorsal rod; VR = ventral rod. Scale bar = 1 µm. **46.** Cross-section through the anterior region of the flagellar pocket showing the fusion of the dorsal and intermediate roots (dr + ir). DR = dorsal rod; VR = ventral rod. Scale bar = 2 µm.

gellar apparatus is shown in Fig. 44–46 from a posterior to anterior view. The dorsal root (dr) originated from the dorsal basal body, and the ventral root (vr) and intermediate root (ir) originated from the ventral basal body. The dorsal root consisted of microtubules that extended towards the anterior end of the cell and initially supported the dorsal side of the flagellar pocket (Fig. 44, 45). The number of microtubules increased as they extended anteriorly along the flagellar pocket and ultimately became the microtubules that subtend the pellicle strips (Fig. 43, 45, 46). The intermediate root, initially formed by four microtubules, was located between the dorsal and the ventral roots, and supported the left side of the flagellar pocket (Fig. 44–46). The number of microtubules in this root increased towards the anterior end of the flagellar pocket, joining the dorsal root in a single microtubular band (dr + ir) that lined the dorsal-left side of the flagellar pocket (Fig. 46). The ventral root originated from the ventral basal body and initially consisted of four microtubules (Fig. 44, 45). Towards the anterior of the cell, the number of these microtubules increased, and eventually reinforced the ventral side of the flagellar pocket and the feeding apparatus (Fig. 46).

Molecular phylogenetic position

The 18S rDNA sequence (2,860 bp) of *H. scaphurum* contained a number of insertions. Two of them were of considerable length: the first one (at position 142 of the sequence) was 567 bp long, and the second (at position 2,122 of the sequence) was 253 bp long. ML and Bayesian analyses of the 39-taxon alignment resulted in identical tree topologies that showed the new isolate clustering within a clade of euglenids consisting of eukaryovorous, primary osmotrophic, and phototrophic species (Fig. 47). The phototrophic and primary osmotrophic euglenids formed two well-supported subclades (ML boostrap value = 83% and Bayesian posterior probability = 1.00 for primary osmotrophs, and ML boostrap value = 99% and Bayesian posterior probability = 1.00 for phototrophic species). The eukaryovorous euglenids *Peranema*, *Aniso-*

nema, *Dinema*, and *H. scaphurum*, however, did not form a distinct clade and instead formed a paraphyletic group.

DISCUSSION

Heteronema scaphurum had all the ultrastructural characteristics distinctive of euglenozoans: a tripartite flagellar root system, flagella with heteromorphic paraxial rods, tubular extrusomes, and mitochondria with discoidal (paddle-shaped) cristae (Simpson 1997; Willey et al. 1988). *Heteronema scaphurum* also had a pellicle with proteinaceous strips, the best synapomorphy for euglenids, and a complex feeding apparatus consisting of rods and vanes that was typical of other eukaryovorous species (e.g. *Peranema* and *Dinema*) (Triemer and Farmer 1991). In agreement with these morphological attributes, our phylogenetic analyses of 18S rDNA sequences robustly placed *H. scaphurum* as a member of the Euglenida and, more specifically, as part of a polytomy formed by all eukaryovorous, primary osmotrophic, and phototrophic euglenids (to the exclusion of the bacterivorous in the analysis).

Heteronema scaphurum was originally described by Skuja in 1934 and later reported in Australian freshwater sites (Schroeckh et al. 2003). These descriptions, however, were solely based on light micrographs. Skuja reported cells with a size range of 78–85 µm, and a diameter of 40–46 µm for *H. scaphurum*, whereas the cells in Australia were shorter (62–75 µm long), more within the range of our isolate (45–70 µm in length and 30 µm in diameter). Both Skuja and Schroeckh et al. described "a characteristic dimple at the posterior end of the cell" (Schroeckh et al. 2003), which we now know is the posterior cytoproct in our isolate. No other data from previous reports (e.g. scanning and transmission electron microscopy or molecular markers) are available, making a more detailed comparison with our isolate impossible. The features observed in our light micrographs, on the other hand, seem to be in accordance with the previous descriptions of this species, persuading us to name our isolate *H. scaphurum*. However, the genus *Heteronema* has
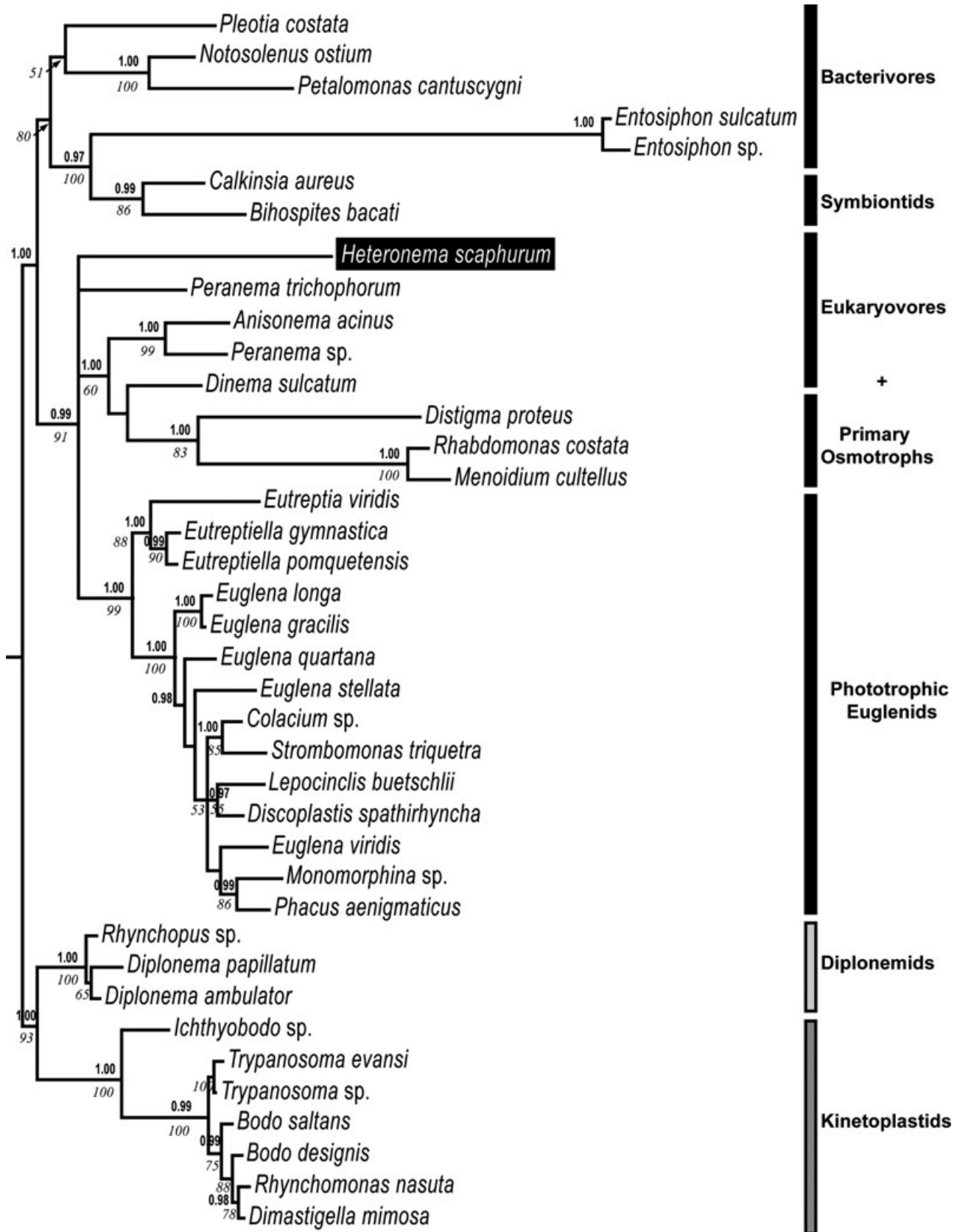
Fig. 47. Maximum likelihood tree, inferred from 39 small subunit (SSU) rDNA sequences showing the molecular phylogenetic position of *Heteronema scaphurum* within euglenid using diplonemid and kinetoplastids as outgroups. The numbers above the stems are Bayesian posterior probabilities over 0.95; ML bootstraps greater than 50% are shown below the stems.

unclear generic limits, largely due to a continuum of variation with other genera, such as *Metanema* and *Dinema* (Larsen and Patterson 1991), coupled with descriptions based solely on light microscopy (Al-Qassab et al. 2002; Lee et al. 2005; Schroeckh et al. 2003). The more comprehensive description of this species reported here using SEM and TEM allows us to demarcate the ultrastructural features of *Heteronema* species more precisely. Moreover, we provide the first molecular data (SSU rDNA sequence) for this genus, which will contribute to a better understanding of euglenid species boundaries.

Pellicle

The eukaryovorous euglenids described so far are capable of euglenoid movement and have helically arranged, delicate pellicle strips that range in total number between 20 and 56 (Leander et al. 2007). Euglenids with less than about 16 strips tend to be rigid and are either bacterivorous, osmotrophic, or phototrophic. *Heteronema scaphurum* has a plastic pellicle formed by 28 helically arranged strips without posterior strip reduction, which is consistent with the range of features present in other eukaryovores. In contrast to other eukaryovores (*Peranema*, *Dinema*, and *Urceolus*), the pellicle strips of *H. scaphurum* were robust in transverse section (100 nm thick) and had distinct overhangs in the articulation zones (Leander and Farmer 2000; Leander et al. 2001b). Unlike *Peranema trichophorum* and *Dinema sulcatum*, *H. scaphurum* did not possess a distinctly shaped "flagellar strip" that holds the ventral (posterior or recurrent) flagellum on the ventral side of the cell during gliding motility (Leander et al. 2001a).

Feeding apparatus

Triemer and Farmer (1991) described four types of feeding apparatuses in euglenids (Types I–IV). Some bacterivores have relatively simple feeding structures consisting of a pocket lined by a row of microtubules (e.g. Type I apparatus in *Petalomonas*), whereas others have a robust and well-developed feeding apparatuses consisting of rods and vanes (e.g. Type II and IV in *Ploeotia* and *Entosiphon* respectively) (Linton and Triemer 1999; Triemer and Farmer 1991; Triemer and Fritz 1987). Eukaryovorous euglenids also have a complex feeding system consisting of a cytostome, four vanes, and two rods formed by varying amounts of supporting microtubules and amorphous matrix (e.g. Type III apparatus in *Dinema* and *Peranema*) (Triemer and Farmer 1991). The feeding apparatus in *H. scaphurum* conforms to Type III in this scheme and is most similar to the apparatus found in *Peranema trichophorum* (Nisbet 1974); the main difference is that the base of the flagellar pocket is more expanded in *H. scaphurum*. Moreover, the rods in *P. trichophorum* are capable of projecting out from the cell to pierce the prey cell during

myzocytosis (Triemer 1997). According to Nisbet (1974), the contraction of longitudinal lamellae attached to the rods is responsible for moving the rods forward. This behaviour was not observed in *H. scaphurum*.

Both *H. scaphurum* and *P. trichophorum* use their two flagella like "arms" to manipulate prey and initiate phagocytosis (Triemer 1997). *Heteronema scaphurum* also secretes a mucilaginous web through the vestibular opening, a novel feature to capture and secure the prey cells (usually several at a time). In both species, the rods move the flagella to one side, preventing the passage of food into the flagellar pocket. The widening of the vestibular opening observed in *H. scaphurum* during phagocytosis also occurs in *P. trichophorum* when it ingests whole cells, although to a much lesser degree; *H. scaphurum* enlarges its anterior end to several times its cell diameter. This has also been observed in other kinds of eukaryotes, such as raptorial ciliates. *Dileptus lamella*, for instance, enlarges its cytostome to a width even wider than that of the prey; *Didinium nasutum* has a fibrous ring that encircles the base of its proboscis and stretches the cell body to accommodate the prey (Verni and Gualtieri 1997). In *H. scaphurum*, the thickenings and the striated fibre around the flagellar pocket might have a similar function. Also, the dorsal and ventral lamellae in *H. scaphurum* might play a role in the expansion of the vestibular opening by pulling from the opposite side of the flagellar pocket.

Faecal pellets in single-celled eukaryotes

After feeding, *H. scaphurum* secretes waste material through the cytoproct, often in the form of faecal pellets. Faecal pellets are found in both marine and fresh-water environments and can vary in size and shape, ranging from minipellets (measuring between 3 μm and 50 μm in diameter) to larger pellets of more than 50 μm (Gowing and Silver 1985). The presence of faecal pellets in sediment samples is usually attributed to meiofunal metazoans, dinoflagellates (Buck and Newton 1995; Buck et al. 1990), ciliates (Stoecker 1984), and radiolarians (Gowing and Silver 1985). This is the first report of any member of the Euglenozoa discharging faecal pellets through a distinct cytoproct.

Ultrastructural identity and phylogenetic position

The SSU rDNA sequence of *H. scaphurum* had an unresolved position among the eukayrovorous species of euglenids. Its ultrastructural characters are consistent with a predator lifestyle (e.g. a feeding apparatus with short rods located in the anterior end of the cell, similar to that of *P. trichophorum*). Shorter rods presumably allow for more flexibility in the posterior two-thirds of the cell which, coupled with a growing number of pellicle strips, would give eukaryovorous euglenids the elasticity to ingest bundles of large prey cells. However, *H. scaphurum* has fewer pellicle

strips than *P. trichophorum* (28 vs. 56), as well as less cell plasticity. The set of morphological characters in *H. scaphurum* is somewhat intermediate between bacterivorous (with fewer pellicle strips but longer rods) and eukaryovores (with more pellicle strips and short rods). Also, *H. scaphurum* shows novel characteristics such as a cytoproct from which small pellets are expelled, and a feeding behaviour that reflects the mechanism by which eukaryovorous ancestors sequestered green algae and ultimately gave rise to phototrophic euglenids (Yamaguchi et al. 2012).

ACKNOWLEDGMENTS

LITERATURE CITED

Al-Qassab, S., Lee, W. J., Murray, S., Simpson, A. G. B. & Patterson, D. J. 2002. Flagellates from stromatolites and surrounding sediments in Shark Bay, Western Australia. *Acta Protozool.*, 41:91–144.

Buck, K. R., Bolt, P. A. & Garrison, D. L. 1990. Phagotrophy and fecal pellet production by an athecate dinoflagellate in Antarctic sea ice. *Mar. Ecol. Prog. Ser.*, 60:75–84.

Buck, K. R. & Newton, J. 1995. Fecal pellet flux in Dabob Bay during a diatom bloom: contribution of microzooplankton. *Limnol. Oceanogr.*, 40:306–315.

Esson, H. J. & Leander, B. S. 2006. A model for the morphogenesis of strip reduction patterns in phototrophic euglenids: evidence for heterochrony in pellicle evolution. *Evol. Dev.*, 8:378–388.

Gibbs, S. P. 1978. The chloroplasts of *Euglena* may have evolved from symbiotic green algae. *Can. J. Bot.*, 56:2883–2889.

Gibbs, S. P. 1981. The chloroplasts of some algal groups may have evolved from endosymbiotic eukaryotic algae. *Ann. N. Y. Acad. Sci.*, 361:193–208.

Gowing, M. M. & Silver, M. W. 1985. Minipellets: a new and abundant size class of marine fecal pellets. *J. Mar. Res.*, 43:395–418.

Guindon, S. & Gascuel, O. 2003. A simple, fast, and accurate algorithm to estimate large phylogenies by maximum likelihood. *Syst. Biol.*, 52:696–704.

Larsen, J. & Patterson, D. J. 1991. The diversity of heterotrophic euglenids. *In*: Patterson, D. J. & Larsen, J. (eds.), The Biology of Free-Living Heterotrophic Flagellates. Systematics Association Special Volume. Claredon Press, Oxford. p. 205–217.

Leander, B. S. & Farmer, M. A. 2000. Comparative morphology of the euglenid pellicle. I. Patterns of strips and pores. *J. Eukaryot. Microbiol.*, 47:469–479.

Leander, B. S. & Farmer, M. A. 2001a. Evolution of Phacus (Euglenophyceae) as inferred from pellicle morphology and SSU rDNA. *J. Phycol.*, 37:143–159.

Leander, B. S. & Farmer, M. A. 2001b. Comparative morphology of the euglenid pellicle. II. Diversity of strip substructure. *J. Eukaryot. Microbiol.*, 48:202–217.

Leander, B. S., Triemer, R. E. & Farmer, M. A. 2001a. Character evolution in heterotrophic euglenids. *Eur. J. Protistol.*, 37:337–356.

Leander, B. S., Witek, R. P. & Farmer, M. A. 2001b. Trends in the evolution of the euglenid pellicle. *Evolution*, 55:2215–2235.

Leander, B. S. 2004. Did trypanosomatid parasites have photosynthetic ancestors? *Trends Microbiol.*, 12:251–258.

Leander, B. S., Esson, H. J. & Breglia, S. A. 2007. Macroevolution of complex cytoskeletal systems in euglenids. *BioEssays*, 29:987–1000.

Lee, W. J., Simpson, A. G. B. & Patterson, D. J. 2005. Free-living heterotrophic flagellates from freshwater sites in Tasmania (Australia), a field survey. *Acta Protozool.*, 44:321–350.

Linton, E. W. & Triemer, R. E. 1999. Reconstruction of the feeding apparatus in Ploeotia costata (Euglenophyta) and its relationship to other euglenoid feeding apparatuses. *J. Phycol.*, 35:313–324.

Milne, I., Lindner, D., Bayer, M., Husmeier, D., McGuire, G., Marshall, D. F. & Wright, F. 2009. TOPALi v2: a rich graphical interface for evolutionary analyses of multiple alignments on HPC clusters and multi-core desktops. *Bioinformatics*, 25:126–127.

Nisbet, B. 1974. An ultrastructural study of the feeding apparatus of *Peranema trichophorum. J. Protozool.*, 21:39–48.

Reynolds, E. S. 1963. The use of lead citrate at high pH as an electron-opaque stain in electron microscopy. *J. Cell Biol.*, 17:208–212.

Rogers, M. B., Gilson, P. R., Su, V., McFadden, G. I. & Keeling, P. J. 2007. The complete chloroplast genome of the chlorarachniophyte *Bigelowiella natans*: evidence for independent origins of chlorarachniophyte and euglenid secondary endosymbionts. *Mol. Biol. Evol.*, 24:54–62.

Ronquist, F. & Huelsenbeck, J. P. 2003. MrBayes 3: Bayesian phylogenetic inference under mixed models. *Bioinformatics*, 19:1572–1574.

Saito, A., Suetomo, Y., Arikawa, M., Omura, G., Khan, S. M. M. K., Kakuta, S., Suzaki, E., Kataoka, K. & Suzaki, T. 2003. Gliding movement in *Peranema trichophorum* is powered by flagellar surface motility. *Cell Motil. Cytoskeleton*, 55:244–253.

Schroeckh, S., Lee, W. J. & Patterson, D. J. 2003. Free-living heterotrophic euglenids from freshwater sites in mainland Australia. *Hydrobiologia*, 493:131–166.

Simpson, A. G. B. 1997. The identity and composition of the Euglenozoa. *Arch. Protistenkd.*, 148:318–327.

Stoecker, D. K. 1984. Particle production by planktonic ciliates. *Limnol. Oceanogr.*, 29:930–940.

Triemer, R. E. & Fritz, L. 1987. Structure and operation of the feeding apparatus in a colorless euglenoid, *Entosiphon sulcatum. J. Protozool.*, 34:39–47.

Triemer, R. E. & Farmer, M. A. 1991. The ultrastructural organization of the heterotrophic euglenids and its evolutionary implications. *In*: Patterson, D. J. & Larsen, J. (eds.), The Biology of Free-Living Heterotrophic Flagellates. The Systematics Association, Oxford. p. 185–204.

Triemer, R. E. 1997. Feeding in *Peranema trichophorum* revisited (Euglenophyta). *J. Phycol.*, 33:649–654.

Triemer, R. E., Linton, E., Shin, W., Nudelman, A., Monfils, A., Bennett, M. & Brosnan, S. 2006. Phylogeny of the Euglenales based upon combined SSU and LSU rDNA sequence comparisons and description of Discoplastis gen. nov. (Euglenophyta). *J. Phycol.*, 42:731–740.

Verni, F. & Gualtieri, P. 1997. Feeding behaviour in ciliated protists. *Micron*, 28:487–504.

Willey, R. L., Walne, P. L. & Kivic, P. A. 1988. Phagotrophy and the origins of the euglenoid flagellates. *Crit. Rev. Plant Sci.*, 7:303–340.

Yamaguchi, A., Yubuki, N. & Leander, B. S. 2012. Morphostasis in a novel eukaryote illuminates the evolutionary transition from phagotrophy to phototrophy: description of *Rapaza viridis* n. gen. et sp. (Euglenozoa, Euglenida). *BMC Evol. Biol.*, 12:29.

[1] Present address: Centre for Comparative Genomics and Evolutionary Bioinformatics, Department of Biochemistry and Molecular Biology, Dalhousie University, 5850 College Street, Halifax, NS, B3H 4R2, Canada